Rapid Communications

Time fractals and discrete scale invariance with trapped ions

Dean Lee, Jacob Watkins, Dillon Frame, Gabriel Given, Rongzheng He, Ning Li, Bing-Nan Lu, and Avik Sarkar
Facility for Rare Isotope Beams and Department of Physics and Astronomy, Michigan State University, Michigan 48824, USA

(Received 1 April 2019; published 24 July 2019)

We show that a one-dimensional chain of trapped ions can be engineered to produce a quantum mechanical system with discrete scale invariance and fractal-like time dependence. By discrete scale invariance we mean a system that replicates itself under a rescaling of distance for some scale factor, and a time fractal is a signal that is invariant under the rescaling of time. These features are reminiscent of the Efimov effect, which has been predicted and observed in bound states of three-body systems. We demonstrate that discrete scale invariance in the trapped ion system can be controlled with two independently tunable parameters. We also discuss the extension to n-body states where the discrete scaling symmetry has an exotic heterogeneous structure. The results we present can be realized using currently available technologies developed for trapped ion quantum systems.

DOI: 10.1103/PhysRevA.100.011403

In this Rapid Communication we show how to construct a one-dimensional system of trapped ions with discrete scale invariance and fractal-like time dependence. In classical systems scale invariance arises when the scale transformation acting on spatial coordinates, $r \to \lambda r$, is a symmetry of the dynamics. This arises naturally if the Hamiltonian transforms homogeneously under rescaling. When the Hamiltonian is quantized, however, this scale invariance cannot persist for bound-state solutions with discrete energy levels. Instead, the scale invariance is broken through a quantum scale anomaly. An analogous effect occurs in relativistic field theories and is responsible for the mass gap in the spectrum of non-Abelian gauge theories such as quantum chromodynamics.

While the quantum scale anomaly spoils invariance under a general scale transformation, it may preserve the symmetry associated with a discrete set of scale transformations. This was first described by Efimov for the bound-state spectrum of three bosons with short-range interactions tuned to infinite scattering length [1–4]. See also Ref. [5] for a review of anomalies in quantum mechanics and the attractive $1/r^2$ potential. Efimov trimers were first observed experimentally through the loss rate of trapped ultracold cesium atoms [6], and a more direct observation has been made using the Coulomb explosion of helium trimers [7]. As the underlying physics is of a universal character, the application and generalization of the Efimov effect has been considered in various settings, including nuclear physics [8,9], bound states with more than three particles [10–14], systems with reduced dimensions [15–17], quantum magnets [18], molecules with spatially varying interactions [19], and Dirac fermions in graphene [20].

We demonstrate that quantum scale anomalies can be produced with trapped ion quantum systems. We start with a one-dimensional chain of ions in a radio-frequency trap with qubits represented by two hyperfine "clock" states. Such systems have been investigated by the trapped ion group at the University of Maryland using $^{171}\mathrm{Yb}^+$ ions [21,22]. Similar efforts have been pioneered by trapped ion groups at ETH Zürich, Freiburg, Innsbruck, Mainz, Stockholm, and the Weizmann Institute. Off-resonant laser beams are used to drive stimulated Raman transitions for all ions in the trap. This induces effective interactions between all qubits with a power-law dependence on separation distance. We define the vacuum state as the state with $\sigma_i^z = 1$ for all i. We use interactions of the form $\sigma_i^x\sigma_j^x + \sigma_i^y\sigma_j^y$, to achieve the hopping of spin excitations. We then use a $\sigma_i^z\sigma_j^z$ interaction to produce a two-body potential felt by pairs of spin excitations, and we also consider an external one-body potential coupled to σ_i^z.

We can view each spin excitation with $\sigma_i^z = -1$ as a bosonic particle at site i with hardcore interactions preventing multiple occupancy. In this language, the Hamiltonian we consider has the form

$$H = \frac{1}{2}\sum_i \sum_{j\neq i} J_{ij}[b_i^\dagger b_j + b_j^\dagger b_i] + \frac{1}{2}\sum_i \sum_{j\neq i} V_{ij} b_i^\dagger b_i b_j^\dagger b_j + \sum_i U_i b_i^\dagger b_i + C, \tag{1}$$

where b_i and $b_i^\dagger$ are annihilation and creation operators for the hardcore bosons on site i. See the Supplemental Material [23] for a derivation of this Hamiltonian. The parameter C is just an overall energy constant. The hopping coefficients J_{ij} have the asymptotic form $J_{ij} = J_0/|r_i - r_j|^\alpha$, where r_i is the position of qubit i. For the purposes of this study, we assume J_{ij} to have exactly this form for $i \neq j$. Similarly, the two-body potential coefficients V_{ij} have the asymptotic form $V_{ij} = V_0/|r_i - r_j|^\beta$. In this work we assume V_{ij} to have exactly this form for $i \neq j$. We consider the case where the lattice of ions is uniform and large, and we start with a constant potential U_i chosen so that bosons with zero momentum have zero energy. Both positive (antiferromagnetic) and negative (ferromagnetic) values can be realized for J_0 and V_0. The exponents α and β can in principle vary in the range between 0 and 3. However, in practice the range between 0.5 and 1.8 is favored in order to enhance coherence times and reduce experimental drifts [22].

We now add to U_i a deep attractive potential at some chosen site i_0 that traps and immobilizes one boson at that site. Without loss of generality, we take the position of that site to be the origin and add a constant to the Hamiltonian so that the energy of the trapped boson is zero. We then consider the dynamics of a second boson that feels the interactions with this fixed boson at the origin. In order to produce a Hamiltonian with classical scale invariance, we choose $\beta = \alpha - 1$. Then at low energies, our low-energy Hamiltonian for the second boson has the form

$$H(p, r) = 2J_0 \sin(\alpha\pi/2)\Gamma(1-\alpha)|p|^{\alpha-1} + \frac{V_0}{|r|^{\alpha-1}}, \quad (2)$$

where we omit corrections of size $O(p^2)$. We are interested in the case where both J_0 and V_0 are negative. In that case we find an infinite tower of even-parity and odd-parity bound states. We label the bound-state energies as $E_+^{(n)}$ and $E_-^{(n)}$, respectively, for non-negative integers n. As expected, our quantized system has a quantum scale anomaly and we are left with two discrete scale symmetries, $r \to \lambda_+ r$ for even parity and $r \to \lambda_- r$ for odd parity. Correspondingly, the bound-state energies follow a simple geometrical progression, $E_+^{(n)} = E_+^{(0)}\lambda_+^{-n}$ and $E_-^{(n)} = E_-^{(0)}\lambda_-^{-n}$. In the Supplemental Material [23] we provide details of the discrete scale invariance for general α. For the special case $\alpha = 2$, the scale factors are $\lambda_\pm = \exp(\pi/\delta_\pm)$, where

$$\delta_+ = \frac{V_0}{J_0\pi}\coth(\delta_+\pi/2), \quad \delta_- = \frac{V_0}{J_0\pi}\tanh(\delta_-\pi/2). \quad (3)$$

In contrast with most other systems with a quantum scale anomaly, we note that the properties of our ion trap system can be tuned using two different adjustable parameters, V_0/J_0 and α. This is convenient for probing a wide range of different phenomena exhibiting discrete scaling symmetry. In the following we will work in lattice units where physical quantities are multiplied by powers of the lattice spacing to make the combination dimensionless and have set $\hbar = 1$. As an example, consider a system with $\alpha = 2$, $\beta = 1$, $J_0 = -1$, and $V_0 = -30$. The wave functions for the first 12 even-parity bound states are shown in Fig. 1. We plot the normalized wave function for $r > 0$. We see clear evidence of discrete scale invariance emerging as we approach zero energy. In Table I we show the energies for the first 14 even-parity and odd-parity bound states and the ratios between consecutive energies. For comparison, at the bottom we show the predictions for these ratios as we approach zero energy at infinite volume. We see that the agreement is quite good.

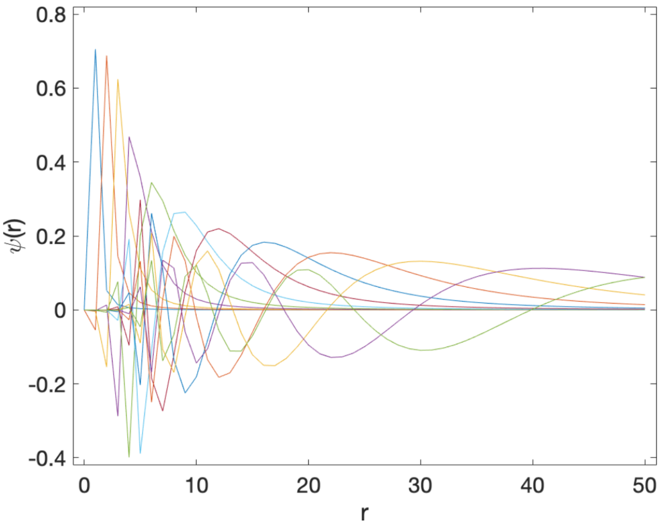

FIG. 1. Bound-state wave functions. Plot of the normalized wave functions for the first 12 even-parity bound states for the case $\alpha = 2$, $\beta = 1$, $J_0 = -1$, and $V_0 = -30$. We plot the region $r > 0$. All quantities are in dimensionless lattice units.

One intriguing question is how discrete scale invariance could persist in quantum many-body systems. It has been demonstrated numerically that the Efimov effect extends beyond bosonic trimers and describes the properties of n-boson systems with the same discrete scaling factor [10–14]. As we will see, something quite different happens in the trapped ion system. Let us start from a particular bound state of the two-body system and ask what happens when we introduce

TABLE I. Bound-state energies. Energies for the first 14 even-parity and odd-parity bound states and ratios between consecutive energies for the case $\alpha = 2$, $\beta = 1$, $J_0 = -1$, and $V_0 = -30$. For comparison we show the theoretical predictions for the ratios λ_+ and λ_- as we approach zero energy at infinite volume.

n	$E_+^{(n)}$	$E_+^{(n-1)}/E_+^{(n)}$	$E_-^{(n)}$	$E_-^{(n-1)}/E_+^{(n)}$
0	−27.05304149		−26.5188669	
1	−11.93067205	2.267520336	−11.79861873	2.247624701
2	−6.977774689	1.709810446	−6.919891389	1.705029468
3	−4.553270276	1.5324754	−4.521425357	1.530466798
4	−3.139972298	1.450098869	−3.120231851	1.449067112
5	−2.233327278	1.405961557	−2.220194049	1.405386998
6	−1.617052389	1.381110033	−1.607920414	1.380786033
7	−1.182654461	1.367307563	−1.176124883	1.367134084
8	−0.869406941	1.360300229	−0.864656962	1.360221377
9	−0.640405903	1.357587332	−0.636916042	1.357568195
10	−0.471738446	1.357544438	−0.469161911	1.357561276
11	−0.347112043	1.359037968	−0.345207121	1.359073675
12	−0.254996818	1.361240684	−0.253589633	1.361282464
13	−0.187011843	1.363532996	−0.18597462	1.363571189
Theory		$\lambda_+ = 1.3895595319$		$\lambda_- = 1.3895595319$

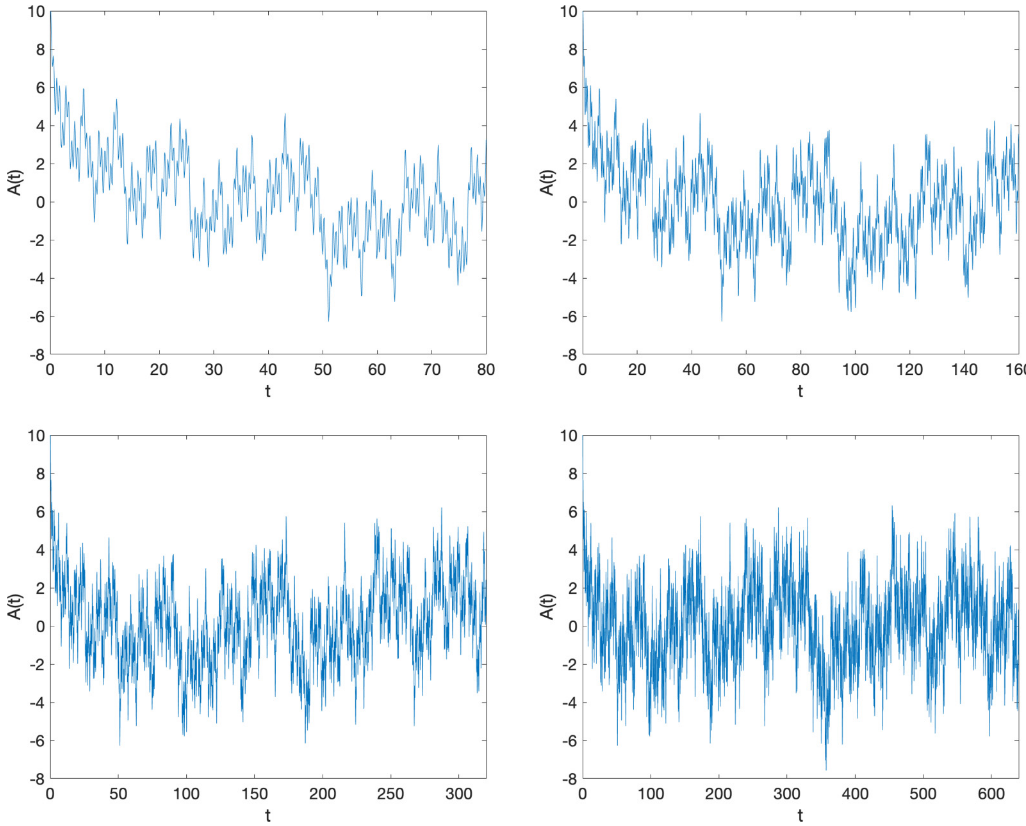

FIG. 2. Time fractals. The amplitude $A(t)$ is displayed over the range from $t = 0$ to 80 in the upper left, $t = 0$ to 160 in the upper right, $t = 0$ to 320 in the lower left, and $t = 0$ to 640 in the lower right. All quantities are in dimensionless lattice units.

a third boson that is weakly bound and very far from the origin. The effective Hamiltonian for the third boson contains a potential energy that is doubled due to interactions of the weakly bound third boson with the two other bosons. As a result of the stronger attractive interaction, the geometric scaling factors $\lambda_\pm$ for the third boson will be smaller than for the two-body system. This argument can be generalized to describe weakly bound states for the general n-body system. The effective potential for the nth boson will be a factor of $n-1$ times larger, and thus the scaling of the n-body energies relative to each $(n-1)$-body threshold is different from the scaling of the k-body bound states for each k between 1 and n. The properties of these exotic systems with heterogeneous discrete invariance will be investigated further in future work.

Let us now consider an initial state $|S\rangle = \sum_{n=0}^{N-1} |\psi_+^{(n)}\rangle$, where we sum over the first N even-parity two-boson bound states $|\psi_+^{(n)}\rangle$ with equal weight. We choose the even-parity states, but we could just as easily choose odd-parity states. The phase convention for each $|\psi_+^{(n)}\rangle$ is chosen so that the tail of the wave function is real and positive at large r. We note that the time-dependent amplitude $A(t) = \mathrm{Re}[\langle S|\exp(-iHt)|S\rangle]$ is invariant under the rescaling $t \to \lambda_+^{\alpha-1} t$, thus endowing it with the properties of a time fractal. The time fractal is particularly interesting for the case when $\lambda_+^{\alpha-1}$ is an integer so that each of the higher frequencies in $A(t)$ are integer multiples of the lower frequencies.

For the case $\alpha = 2$ and $J_0 = -1$, we can produce the time scaling factor $\lambda_+^{\alpha-1} = \lambda_+ = 2$ by setting $V_0 = -14.238\,829\,3$. In Fig. 2 we show the amplitude $A(t)$ ranging from $t = 0$ to 80 in the upper left, $t = 0$ to 160 in the upper right, $t = 0$ to 320 in the lower left, and $t = 0$ to 640 in the lower right. Aside from small deviations, we see that the time dependence shows fractal-like self-similarity when we zoom in or out by a scale factor very close to 2. The best fit for the scale factor is approximately 1.9. In the Supplemental Material [23] we show how a time fractal can be realized experimentally using quantum interference on a trapped ion quantum system.

The time fractals that we have discussed are closely related to the Weierstrass function $w(x) = \sum_{n=0}^{\infty} a^n \cos(b^n \pi x)$. Weierstrass showed that this function is continuous everywhere but differentiable nowhere when $0 < a < 1$, b is an odd integer, and $ab > 1 + 3\pi/2$ [24]. Hardy extended the proof to any $0 < a < 1 < b$ and $ab \geqslant 1$ [25]. We note that $aw(bx)$ equals $w(x)$ plus the smooth function $\cos(\pi x)$, and this suggests that the fractal dimension of the Weierstrass function should given by [26]

$$D = 2 + \frac{\log a}{\log b}. \tag{4}$$

This result for the fractal dimension is confirmed by the box-counting method for determining fractal dimensions [27].

Our initial state $|S\rangle = \sum_{n=0}^{N-1} |\psi_+^{(n)}\rangle$ produces the fractal-like amplitude

$$A(t) = \sum_{n=0}^{N-1} \cos(E_+^{(n)} t) = \sum_{n=0}^{N-1} \cos(\epsilon_+ \lambda_+^{-n} t). \tag{5}$$

In the limit of large N, our choice of parameters corresponds to the limiting case $a \to 1$ and $b = \lambda_+$, with $x = \epsilon_+ \lambda_+^{-N+1} t/\pi$. Therefore, the fractal dimension for our time fractal will be $D = 2$. If we instead choose the initial state to have the form $|S(a)\rangle = \sum_{n=0}^{N-1} a^{n/2} |\psi_+^{(n)}\rangle$ for $a < 1$, then in the limit $N \to \infty$, the fractal dimension will be

$$D = 2 + \frac{\log a}{\log \lambda_+}. \tag{6}$$

There are many interesting related phenomena that one can explore in connection with time fractals and the dynamics of systems with discrete scale invariance. One fascinating topic is the adiabatic evolution of a system with discrete invariance as the interactions are varied slowly. Another is the response of a system with discrete scale invariance when driven in resonance with one of its bound state energies. In this Rapid Communication we have shown that the intrinsic power-law interactions of the trapped ion system make it an ideal system for exploring the physics of quantum scale anomalies, discrete scale invariance, and time fractals. There are clearly many directions that one can explore in this new area, and we look forward to working with others to develop further applications and experimental realizations of many of these concepts.

We are grateful for discussions with Zohreh Davoudi, Chao Gao, Pavel Lougovski, Titus Morris, Thomas Papenbrock, and Raphael Pooser. We acknowledge financial support from the U.S. Department of Energy (DE-SC0018638 and DE-AC52-06NA25396). Computational resources were provided by the Julich Supercomputing Centre at Forschungszentrum Jülich, Oak Ridge Leadership Computing Facility, RWTH Aachen, and Michigan State University.

[1] V. N. Efimov, Sov. J. Nucl. Phys. **12**, 589 (1971).
[2] V. N. Efimov, Phys. Rev. C **47**, 1876 (1993).
[3] P. F. Bedaque, H.-W. Hammer, and U. van Kolck, Phys. Rev. Lett. **82**, 463 (1999).
[4] P. F. Bedaque, H.-W. Hammer, and U. van Kolck, Nucl. Phys. A **646**, 444 (1999).
[5] S. A. Coon and B. R. Holstein, Am. J. Phys. **70**, 513 (2002).
[6] T. Kraemer, M. Mark, P. Waldburger, J. G. Danzl, C. Chin, B. Engeser, A. D. Lange, K. Pilch, A. Jaakkola, H.-C. Naegerl *et al.*, Nature (London) **440**, 315 (2006).
[7] M. Kunitski *et al.*, Science **348**, 551 (2015).
[8] P. F. Bedaque, H.-W. Hammer, and U. van Kolck, Nucl. Phys. A **676**, 357 (2000).
[9] G. Hagen, P. Hagen, H. W. Hammer, and L. Platter, Phys. Rev. Lett. **111**, 132501 (2013).
[10] L. Platter, H.-W. Hammer, and U.-G. Meißner, Phys. Rev. A **70**, 052101 (2004).
[11] H. W. Hammer and L. Platter, Eur. Phys. J. A **32**, 113 (2007).
[12] J. von Stecher, J. P. D'Incao, and C. H. Greene, Nat. Phys. **5**, 417 (2009).
[13] J. von Stecher, Phys. Rev. Lett. **107**, 200402 (2011).
[14] J. Carlson, S. Gandolfi, U. van Kolck, and S. A. Vitiello, Phys. Rev. Lett. **119**, 223002 (2017).
[15] Y. Nishida and S. Tan, Few Body Syst. **51**, 191 (2011).
[16] Y. Nishida, S. Moroz, and D. T. Son, Phys. Rev. Lett. **110**, 235301 (2013).
[17] L. Happ, M. Zimmermann, S. I. Betelu, W. P. Schleich, and M. A. Efremov, arXiv:1904.07544.
[18] Y. Nishida, Y. Kato, and C. D. Batista, Nat. Phys. **9**, 93 (2013).
[19] Y. Nishida and D. Lee, Phys. Rev. A **86**, 032706 (2012).
[20] O. Ovdat, J. Mao, Y. Jiang, E. Y. Andrei, and E. Akkermans, Nat. Commun. **8**, 507 (2017).
[21] J. Zhang, P. W. Hess, A. Kyprianidis, P. Becker, A. Lee, J. Smith, G. Pagano, I. D. Potirniche, A. C. Potter, A. Vishwanath *et al.*, Nature (London) **543**, 217 (2017).
[22] J. Zhang, G. Pagano, P. W. Hess, A. Kyprianidis, P. Becker, H. Kaplan, A. V. Gorshkov, Z. X. Gong, and C. Monroe, Nature (London) **551**, 601 (2017).
[23] See Supplemental Material at http://link.aps.org/supplemental/10.1103/PhysRevA.100.011403 for details on the Hamiltonian, dispersion relation, two-body system, and realization of time fractals.
[24] K. Weierstrass, *Abhandlungen aus der Functionenlehre* (Springer, Berlin, 1886).
[25] G. H. Hardy, Trans. Am. Math. Soc. **17**, 301 (1916).
[26] B. R. Hunt, Proc. Am. Math. Soc. **126**, 791 (1998).
[27] J. L. Kaplan, J. Mallet-Paret, and J. A. Yorke, Ergod. Theor. Dyn. Syst. **4**, 261 (1984).